REPORT DOCUMENTATION PAGE

Form Approved
OMB No. 0704-0188

1. REPORT DATE *(DD-MM-YYYY)*	2. REPORT TYPE	3. DATES COVERED *(From - To)*
12-06-2007	Journal Article	

4. TITLE AND SUBTITLE

The Impact of Manifold-to-Orifice Turning Angle on Sharp-Edge Orifice Flow Characteristics in both Cavitation and Non-Cavitation Turbulent Flow Regimes (Preprint)

5a. CONTRACT NUMBER

5b. GRANT NUMBER

5c. PROGRAM ELEMENT NUMBER

6. AUTHOR(S)
W.H. Nurick & T. Ohanian (Science and Technology Applications LLC);
D.G. Talley & P.A. Strakey (AFRL/PRSA)

5d. PROJECT NUMBER

5e. TASK NUMBER
50260538

5f. WORK UNIT NUMBER

7. PERFORMING ORGANIZATION NAME(S) AND ADDRESS(ES)

Air Force Research Laboratory (AFMC)
AFRL/PRSA
10 E. Saturn Blvd.
Edwards AFB CA 93524-7680

8. PERFORMING ORGANIZATION REPORT NUMBER

AFRL-PR-ED-JA-2007-325

9. SPONSORING / MONITORING AGENCY NAME(S) AND ADDRESS(ES)

Air Force Research Laboratory (AFMC)
AFRL/PRS
5 Pollux Drive
Edwards AFB CA 93524-7048

10. SPONSOR/MONITOR'S ACRONYM(S)

11. SPONSOR/MONITOR'S NUMBER(S)
AFRL-PR-ED-JA-2007-325

12. DISTRIBUTION / AVAILABILITY STATEMENT

Approved for public release; distribution unlimited (PA #07234A).

13. SUPPLEMENTARY NOTES
Submitted for publication in *Journal of Spacecraft and Rockets*..

14. ABSTRACT

The approach taken was to analyze the results in a manner consistent with application by design engineers to new and existing applications, while providing some insight into the processes that are occurring. This paper deals with predicting the initiation of cavitation, cavitation impacts on Cc, and non-cavitation impacts on Cd from L/D of 5 sharp-edge orifices with both single angle and compound angle directional flow. The results show that in the cavitation regime, Cc is controlled by the cavitation number, where the data follows the power with Kcav, and inception of cavitation occurs at a Kcav of 1.8. In the non-cavitation regime Cd is controlled by Reynolds number, and the head loss coefficient, KL for all angles is a function of the manifold-to-orifice velocity ratio. Compound angle orifices Cc and KL were found to be influenced more by the initial turning angle than the orifice turning angle. In the non-cavitation regime for conditions where the cross velocity is 0 the data are consistent with the first order equation relating HL to the dynamic pressure where KL is constant, which is consistent with in-line orifices.

15. SUBJECT TERMS

16. SECURITY CLASSIFICATION OF:			17. LIMITATION OF ABSTRACT	18. NUMBER OF PAGES	19a. NAME OF RESPONSIBLE PERSON
					Dr. Douglas Talley
a. REPORT	b. ABSTRACT	c. THIS PAGE			19b. TELEPHONE NUMBER *(include area code)*
Unclassified	**Unclassified**	**Unclassified**	SAR	21	N/A

Standard Form 298 (Rev. 8-98)
Prescribed by ANSI Std. 239.18

THE IMPACT OF MANIFOLD-TO-ORIFICE TURNING ANGLE ON SHARP-EDGE ORIFICE FLOW CHARACTERISTICS IN BOTH CAVITATION AND NON-CAVITATION TURBULENT FLOW REGIMES (preprint)

By:

W. H. Nurick & T. Ohanian
Science & Technology Applications LLC (STA)
Moorpark, CA

And

D.G. Talley & P. A. Strakey
Air Force Research Laboratory
Edwards Air Force Base CA

ABSTRACT

The approach taken was to analyze the results in a manner consistent with application by design engineers to new and existing applications, while providing some insight into the processes that are occurring. This paper deals with predicting the initiation of cavitation, cavitation impacts on C_c, and non-cavitation impacts on C_d from L/D of 5 sharp-edge orifices with both single angle and compound angle directional flow. The results show that in the cavitation regime, C_c is controlled by the cavitation number, where the data follows the ½ power with Kcav, and inception of cavitation occurs at a Kcav of 1.8. In the non-cavitation regime C_d is controlled by Reynolds number, and the head loss coefficient, K_L for all angles is a function of the manifold-to-orifice velocity ratio. Compound angle orifices C_c and K_L were found to be influenced more by the initial turning angle than the orifice turning angle. In the non-cavitation regime for conditions where the cross velocity is 0 the data are consistent with the first order equation relating H_L to the dynamic pressure where K_L is constant, which is consistent with in-line orifices.

INTRODUCTION

For application to rocket engine injectors, cavitation can occur in the entrance from flow passages into sharp-edge orifices. The actual onset of cavitation depends on the orifice edge sharpness, L/D, upstream pressure, cross velocity, orifice entrance angle, and back pressure. In application where the engine is "deep" throttled cavitation can occur if the chamber pressure is sufficiently low and/or the upstream flow causes a contraction/expansion to support separation. The inability to predict the occurrence of cavitation can lead to a catastrophic failure of an engine and loss of mission.

In 1976 Nurick[1] published a paper discussing cavitation for in-line sharp-edge orifices and proposed a simple 1st order model for predicting cavitation. Photographic evidence was also presented showing that after the inception of cavitation, the vena-contracta reattachment point started to move downstream toward the exit of the orifice. This also resulted in a decrease in discharge coefficient (C_d) until it reached the separation value. In some cases the orifice remained attached even at a cavitation number of 1 while in other cases hydraulic flip occurred in the region of K_{cav} of 1.3 or less. In 2007 Nurick, Ohanian, Talley and Strakey[2] (to be published) wrote a paper specifically dealing with sharp edged orifices having a 90 degree orientation relative to the manifold feed. This study revealed that the simple relationship could be extended to 90 degree orifices in cross flow although the C_c and K_L relationships needed to account for the manifold to orifice velocity ratio.

The early Nurick[1] results were subsequently utilized in other studies[3, 4, 5] that included CFD modeling to extend model applicability and in some cases verify codes. In the last 10-15 years CFD modeling has improved considerably and predictions are now being made that show the impact of key design/operating variables on both the discharge coefficient (C_d) and contraction coefficient (C_c). Unfortunately, there is little if any test data that can be utilized to verify these predictions. It is the hope of the authors that the results presented in this paper will be useful in that goal.

This paper is an extension of the earlier work[1, 2] and includes varying the turning angle from as low as 60^o up to 120^o, for an orifice L/D of 5. The approach taken in this paper is to present the results in a manner consistent with application by design engineers to new and existing applications, while providing some insight into the processes that are occurring. This paper deals with predicting the initiation of cavitation and the impact of the variables listed above on C_c, C_d, and K_L. In addition the impact of the same variables in the turbulent flow regime is also discussed and correlations are provided.

TEST FACILITY AND TEST SETUP

FACILITY DESIGN

The experimental investigation was carried out at the Air Force Research Laboratory cold-flow injector characterization facility, a simplified schematic of which is shown in Figure 1. Water, which is used as a simulant for liquid oxygen, is stored and pressurized

in a 35 ft^3 tank. The injector inlet flow rate is controlled with a throttling valve and measured with one of several turbine flow meters arranged in parallel to cover a wide range of flow rates. Downstream of the injector, another turbine flow meter measures the outlet flow rate and a back-pressure regulator maintains the injector fluid pressure. Fluid pressures of up to 1500 lb/in^2 and manifold velocities up to 130 f/s may be produced in this manner. The injector, as illustrated in Figure 2, consists of an interchangeable stainless steel plate with a sharp-edged hole machined in the center of the plate. This is mounted against the fluid manifold, which contains a 0.25 in square channel machined into the manifold. A plenum and screen at the inlet and exit of the manifold reduces the velocity before the flow enters the manifold in order to generate a reproducible flow field at the entrance to the orifice. The distance from the manifold inlet screen to the orifice entrance is 2.5 in or 9 manifold channel widths. The entire arrangement is secured inside an optically accessible pressure chamber which is rated to 2000 psi.

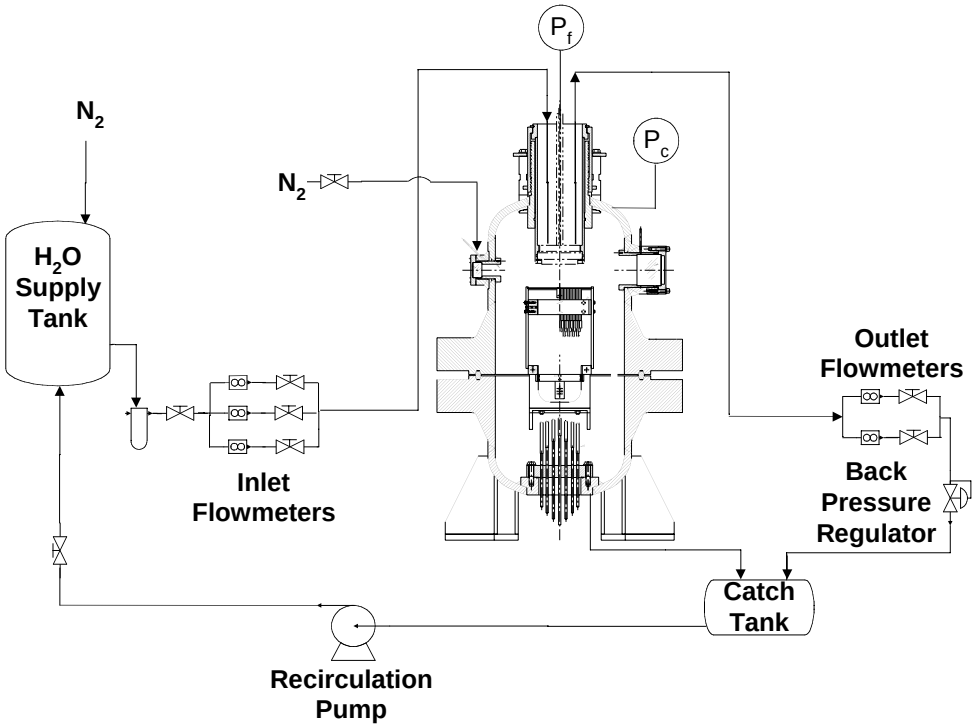

Figure 1 - Schematic of AFRL Cold Flow Test Facility

The orifices are either pilot drilled and reamed, or made by electrical discharge machining with a diameter tolerance of +/- 13 μm and inlet edge radius to orifice diameter ratio of less than .003, ensuring a sharp edged inlet. Chamber pressure, orifice pressure-drop, and inlet and outlet flow rates are recorded by a 12 bit analog to digital conversion board and the data is stored on a personal computer. Experiments are typically conducted by setting the fluid pressure and flow rates to a predetermined value, with the chamber pressure being gradually increased while the data acquisition system records flow rates and pressures. This allows for a large amount of data to be collected in

a relatively short period of time. Orifice pressure drop and chamber gas pressure are measured within an accuracy of +/- 0.25%. Manifold velocities are held constant to within +/- 1.5% during the experiment. Because of the difficulty associated with directly

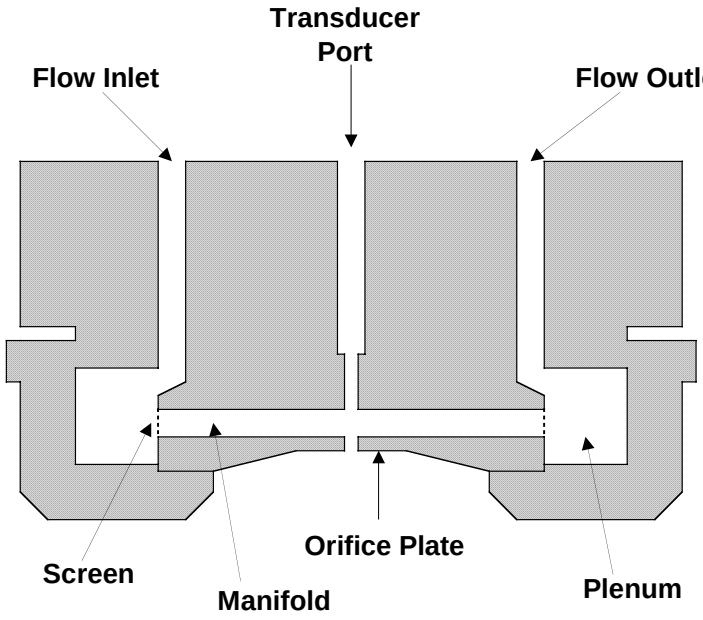

Figure 2 - Injector Schematic

measuring the orifice flow rate inside of the pressurized vessel, the orifice flow rate is measured by subtracting the manifold outlet flow rate from the manifold inlet flow rate. The experimental error associated with the discharge coefficient measurement is limited by the accuracy of the flow meters which is +/- 0.5%. This translates to an error on the discharge coefficient data of about +/- 0.5% at the lowest manifold flow rates and highest orifice flow rates, to +/- 10% at the lowest orifice flow rates and highest manifold flows. A typical error for the intermediate flow rates is on the order of +/- 4%.

MANIFOLD CONFIGURATION

For the data in this paper the manifold was operated such that fluid enters the inlet port and a portion of the flow exits the manifold and the remainder enters the orifice. A sketch of the configuration is shown in Figure 3.

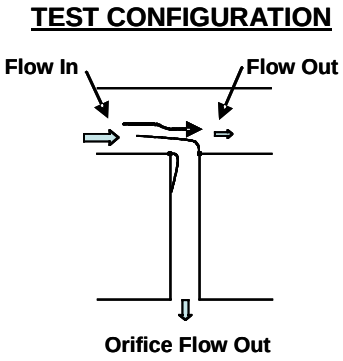

Figure 3 – Manifold / Orifice Entrance Test Configuration

ORIFICE CONFIGURATIONS

Both single and compound angle orifice designs were tested. As shown in Figure 4 below, for the single angle direction feed, the orifice is oriented such that the flow enters the orifice by turning in the direction of its angle; while for the compound angle direction flow the flow must first turn 90^o then immediately turn in the direction of the orifice angle.

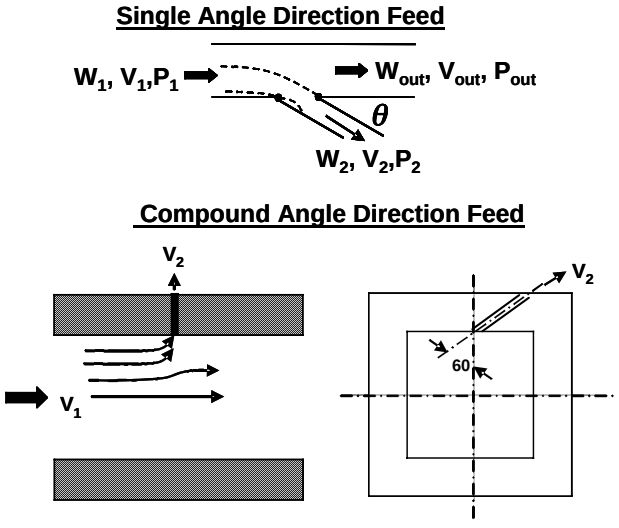

Figure 4 - Illustration of Flow Turning For Both Single & Compound Angle Orifices

The range of operating conditions and orifice geometries typical of liquid rocket injectors was studied and are given in Table 1.

Table 1 - Test Variables and Range of Testing

Orifice Diameter (in)	0.0468 - .0839
Length to Diameter Ratio	3 - 10
Fluid Pressure (psi)	100 - 1500
Back-Pressure (psi)	13.05 - 1500
Cross-Velocity (f/s)	0 – 60.7
Orifice Re_d	$1.0x10^4$ - $3.0x10^5$
Manifold Re_w	$6.0x10^3$
Manifold Dynamic Head to Orifice Static Dp Ratio	$5.0x10^{-5}$ - $6.0x10^0$

ANALYSIS APPROACH

CAVITATION REGIME (TURBULENT FLOW)

The definition of cavitation number should take into account all the dynamic variables that impact the process. For high Re number flow C_c is also a function of A_2/A_1 and therefore the cavitation number should include the manifold contraction, any flow turning as well as the processes to the exit. Consistent with this the definition of cavitation number utilized in this study is stated as:

$$K_{cav} = \frac{P_1 - P_v}{P_1 - P_2} \qquad (1)$$

The derivation of relationships between C_d and C_c depend on various assumptions unique to the flow characteristics of the configuration tested. For the tests in this program the manifold velocity can not be neglected in the derivation of discharge coefficient. For this case the discharge coefficient is defined as:

$$C_d = \frac{V_2}{\left[(2g/\rho)(P_1 - P_2) + V_1^2\right]^{1/2}} \qquad (2)$$

Combining Equations 1 and 2 in addition to the Bernoulli equation with the assumption that the head loss between the manifold and the vena-contracta is small results in Equation 3:

$$C_d = \frac{C_c K_{cav}^{1/2}}{\left[\frac{(V_1 - V_{out})^2}{V_2^2}\left(\frac{A_1}{A_2}\right)^2 + \left(\frac{V_1}{V_2}\right)^2 C_c^2 (K_{cav} - 1)\right]^{1/2}} \qquad (3)$$

For conditions where all the manifold flow enters the orifice Equation 3 reduces to:

$$C_d = \frac{C_c K_{cav}^{1/2}}{\left[1 + \left(\frac{A_2}{A_1}\right)^2 C_c^{\,2}\left(K_{cav} - 1\right)\right]^{1/2}} \qquad (4)$$

And for in-line orifices where $V_1 << V_2$ and $V_{out} = 0$:

$$C_d = \frac{C_c \left(K_{cav}\right)^{1/2}}{\left[1 - \left(\frac{A_2}{A_1}\right)^2 Cc^2\right]^{1/2}} \qquad (5)$$

Then when the product of area ratio times C_c squared is small with respect to 1 this reduces to:

$$C_d = C_c K_{cav}^{1/2} \qquad (6)$$

This expression was used in the early Nurick[1] study and subsequently adopted by others.

NON-CAVITATION REGIME (TURBULENT FLOW)

In basic fluid dynamics texts, flow around bends is defined by a loss coefficient which is included in the specification of overall head loss. Consistent with this tradition the data in the non-cavitation turbulent flow is both analyzed and correlated in terms of the impact on overall head loss. Based on constant velocity studies where turning angle has been varied the loss coefficient has been found to be a function of the turning angle. Therefore, the loss coefficient (K_L) is defined by:

$$H_L = K_L(\theta)\frac{\rho}{2g} V_2^{\,2} \qquad (7)$$

For conditions where the velocity is not constant then K_L should also be a function of V_1/V_2 or:

$$H_L = K_L\left(\theta, \frac{V_1}{V_2}\right)\frac{\rho}{2g} V_2^{\,2} \qquad (8)$$

The Bernoulli equation was used to define H_L:

$$H_L = (P_1 - P_2) + \frac{\rho}{2g}(V_1^{\,2} - V_2^{\,2}) \qquad (9)$$

RESULTS AND DISCUSSION

CAVITATION REGIME

It is important to first define the flow regimes so that the data can be related to specific processes. There are three flow regimes of interest in the cavitation regime. The first is the onset of cavitation (inception of cavitation) where bubbles are formed at the orifice entrance and continue to flow downstream until they are converted back to liquid in the recovery area. The second is full cavitation where the bubbles coalesce forming a vapor cavity whose length varies as the cavitation number is lowered. The third is supercavitation where the vapor pocket attachment has moved to the orifice exit and beyond but the flow still acts as attached. For this study only the 90 degree orifice angle configuration experienced supercavitation. For all other angles it did not appear to occur. The physical reason is unknown at this time and its determination would require additional measurements including photographic evidence of the vapor cavity characteristics.

All three of these regimes, in addition to separation, are illustrated in Figure 5. Note that hydraulic flip can occur at any point in the cavitation regime depending on the orifice L/D as well as flow conditions. There also appears to be potential for "hysteresis" to also occur at start-up as indicated by the two identical run conditions shown in Figure 5. Note that in one case the orifice was separated at the outset but at about the point were cavitation inception occurs it immediately flips to the non-cavitation condition. In the other test it appears that the flow is attached at the onset but not in separation since the data curves upward until about a K_{cav} of 1.17 where C_c becomes constant and then, as is normal, transitions to the non-cavitation condition. The transition zone is however impacted by the ability of the flow to remain attached and other processes most likely occurring at the orifice exit. These resulting impacts on the cavitation characteristics are noted in Figure 5 by variable C_c. Also shown is the constant C_c condition here the flow smoothly transitions from non-cavitation to cavitation and remains attached. This later condition is the basis for the correlation presented in this paper

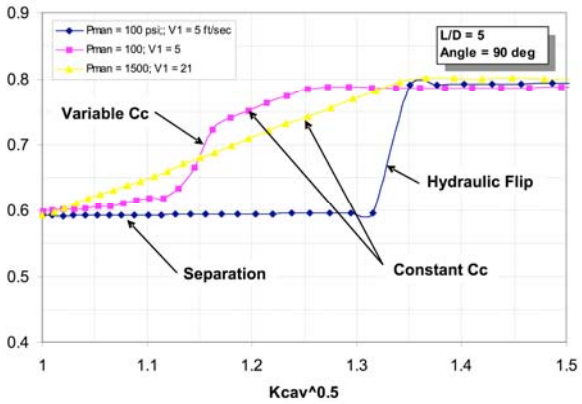

Figure 5 - Sharp-Edge Orifice Data Depicting All Flow Regimes

Single Angle Direction

Inception of Cavitation - The inception of cavitation occurs where the discharge coefficient either abruptly changes to a decreasing value with decreasing cavitation number or more smoothly transitions, both resulting in a constant slope consistent with Equation 3. Both characteristics are illustrated in Figure 6. Interestingly the cavitation data all follow the relationship of Equation 3 suggesting that the denominator for a given test is constant. This is not unexpected since the tests were run such that the velocity ratio (V1/V2) remained constant for a given test.

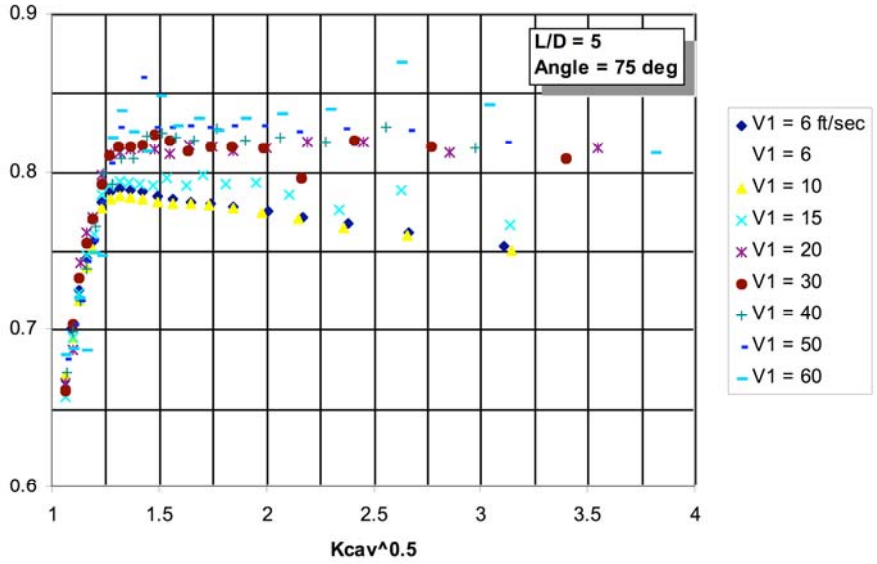

Figure 6 - Cavitation Number Vs Discharge Coefficient

For each test sequence, where the upstream conditions were set and the back pressure systematically lowered, the data were analyzed to determine the point where the data deviated from the straight line relationship. This is also the point where the flow is no longer choked and transitions into the non-cavitation turbulent regime. Analysis of the data revealed that the cavitation number where cavitation inception begins remains constant (within experimental error) at all conditions regardless of turning angle or upstream conditions at K_{cav} ~ 1.8. In some cases there is a transition region where Cc varies until the flow fully chokes and C_c remains constant. When this occurs C_c becomes constant at K_{cav} between ~ 1.5-1.6.

Full Cavitation – Since the impact of upstream conditions on the contraction coefficient should be related to the non-symmetric nature of the flow due to acceleration from bending as well as both area reduction and attachment on the far wall. These characteristics should impact the vena-contracta formation process. Equation 3 can be solved for Cc and the result is:

$$C_c = \frac{a}{\left(\frac{K_{cav}}{C_d^{\,2}} - b\right)^{1/2}} \qquad (10)$$

Where: $a = \left(\frac{V_1 - V_{out}}{V_2}\right)\left(\frac{A_1}{A_2}\right)$ (11)

$$b = \left(\frac{V_1}{V_2}\right)^2 \left(K_{cav} - 1\right) \qquad (12)$$

Therefore it is expected that C_c will be a function of the velocity ratio (area ratio is constant for these tests and the ratio V_{out}/V_2 is dependent on V_1/V_2). For different turning angles it would be expected that C_c would also be a function of angle. The contraction coefficient is therefore a function of:

$$C_c = f[\theta, V_1/V_2] \qquad (13)$$

For a given orifice the tests were conducted at a constant velocity ratio, and since the area ratio is small it would be expected that the contraction ratio would follow the Equation 6 relationship. To test this hypothesis all data were first evaluated according to Equation 6 and typical results are presented in Figure 7.

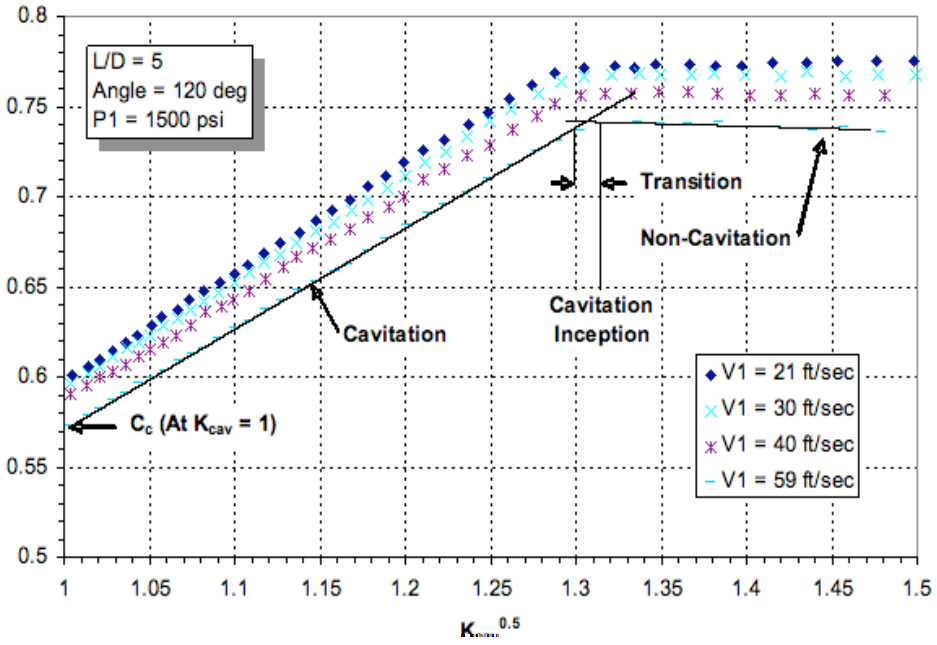

Figure 7 – Typical Test Results Plotted According to Equation 6

These results and in fact all test data show the same trend that confirm that the contraction ratio is a function of both turning angle and velocity ratio.

Even though it would be expected that using Equation 4 or Equation 6 would yield near identical results the test data was reduced to define C_c using Equation 10 for each turning angle. The results are plotted in Figure 8 as a function of V_1/V_2. For the 60^o turning angle the results show that C_c initially increases with velocity ratio then decreases similar to that of the other angles. As the manifold exit flow rate approaches zero the Cc appears to "sense" the resistance of a wall being formed and therefore seek the value for no exit flow.

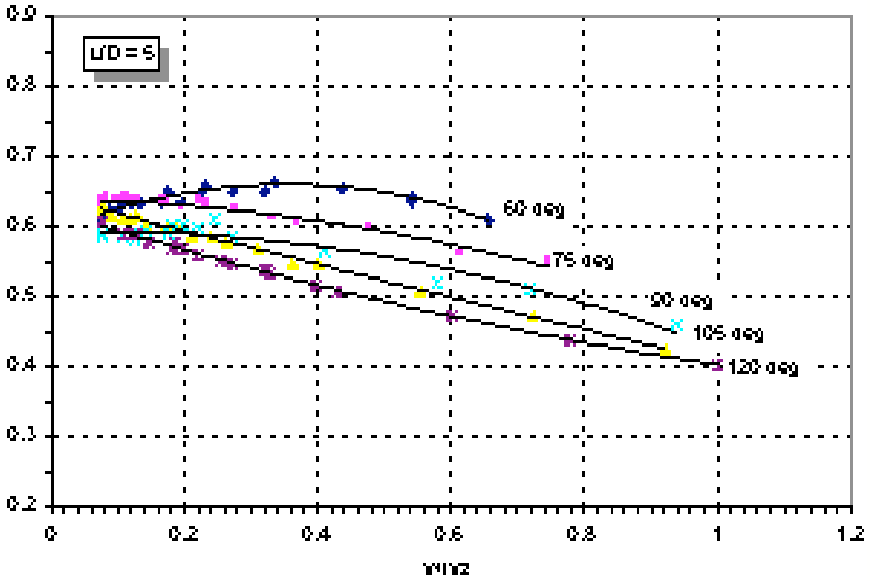

Figure 8 - Impact of Cross Velocity and Turning Angle on C_c

The significant impact of turning angle and velocity ratio on Cc suggests that increasing either variable results in a decrease in the vena-contracta area. This further suggests that the ability of the accelerating flow to reach vapor pressure increases as the flow turning angle and/or the velocity ratio increases. This decrease in the vena-contracta area increases the vapor area. A hypothesis for this phenomenon is that it is related to the dynamics of the flow impacting on the far wall creating a vapor pocket only on the near wall. Best-fit curves were fit to each angle in the form:

$$C_c = A\left(\frac{V_1}{V_2}\right)^2 + B\frac{V_1}{V_2} + C \qquad (14)$$

The constants for each angle are given in Table 2

Table 2 - Constants for Equations 14

Angle	A	B	C	R^2
60	-0.5418	0.3829	0.5931	0.8717
75	-0.1508	-0.0180	0.6403	0.9458
90	-0.1846	0.0202	0.5940	0.9211
105	0.0155	-0.2506	0.6447	0.9945
120	0.0825	-0.3034	0.6250	0.9916

Application of this equation is only valid within the limits of the data as indicated in Figure 8.

Utilizing the results from the cavitation study for analysis and design is straight forward. For example, given an orifice and manifold design as well as the expected operating conditions, K_{cav} can be calculated using Equation 1. The value of K_{cav} can then be compared with that required to achieve incipient cavitation (i.e. 1.8) and if equal to or less than this value operation will be in the cavitation regime. Then based on the design variables such as; (1) manifold/orifice area ratio, (2) flow rate ratio and (3) turning angle, C_c can be calculated using Equation 14. The orifice discharge coefficient can then be calculated from Equation 10.

It is important to note that since the area ratio was not varied, the equations have only been validated at the ratio A_2/A_1 used in this study. However, the area ratio of this study was sufficiently small that it could be neglected. Therefore Equation 14 has only been validated when the area ratio can be neglected. For this case Equation 6 could also be used to define C_d.

Compound Angle Direction Feed

Inception of Cavitation - The designation of 90_xx for the compound angle orifices designates the flow must first turn 90 degrees and then turn in the direction of the orifice angle (xx).

The compound angle direction feed data, Figure 9, followed the identical trends as the single angle direction feed data. Within the experimental accuracy, cavitation inception was between 1.7 and 1.8 as shown in Figure 9 ($K_{cav}^{1/2}$ = 1.3 to 1.34). The inception of cavitation for both the 90_60 and 90_75 degree data again is taken at the beginning of the rollover from the turbulent regime to the cavitation regime. It should be noted that full cavitation is not achieved until ~ $K_{cav}^{1/2}$ =1.3. The sharp decline in Cd in the non-cavitation regime is due to the definition of C_d that includes V_1.

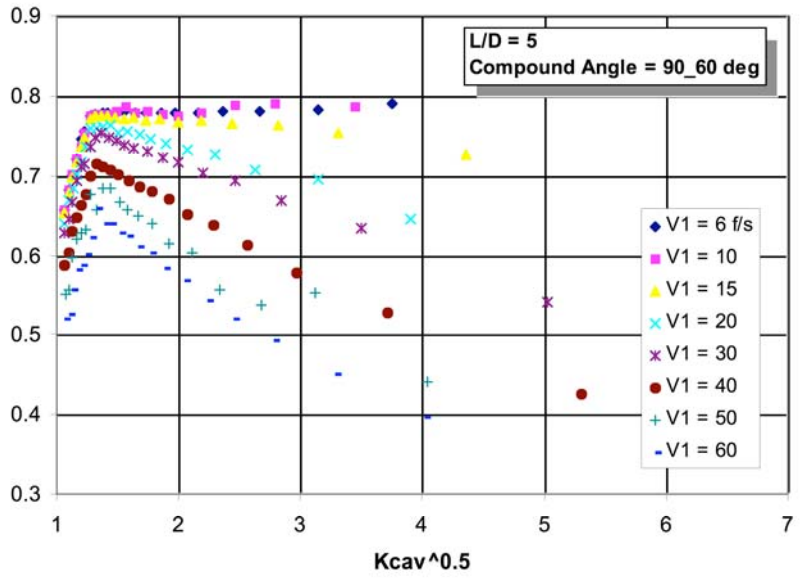

Figure 9 - C_d Vs Cavitation Number for Compound Angle 90_60 Deg.

Full Cavitation - The variation in the contraction coefficient with velocity ratio for the compound angle direction feed is shown in Figure 10. The data are compared with the single angle direction feed data of 60 and 75 degrees. Note that both the 90_60 and the 90_75 data nearly fit to a single curve. In addition note that as the manifold exit flow rate approaches zero the Cc tends to approach a constant at a value equal to that determined for the approach velocity case.

Since there are only two compound angle configurations tested individual equations are provided. The equation is:

$$C_c = A\left(\frac{V_1}{V_2}\right)^2 + B\frac{V_1}{V_2} + C \qquad (15)$$

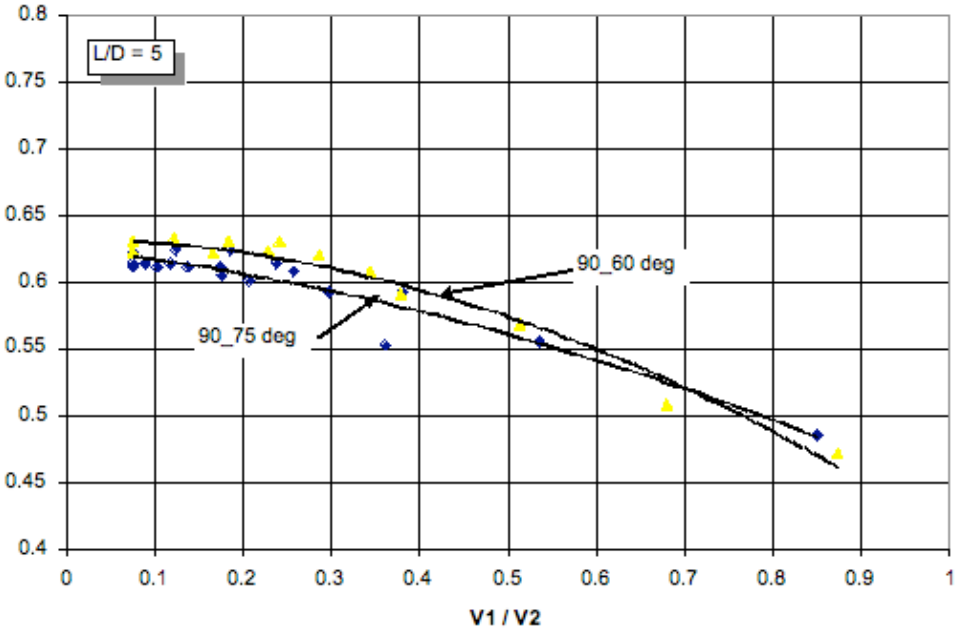

Figure 10 - Impact of Manifold-to-Orifice Velocity Ratio on C_c

The constants for each configuration are provided in Table 3.

Table 3 - Constants for Equation 15

Angle	A	B	C
90_60	-0.2125	-0.0.114	0.6324
90_75	-0.1058	-0.0771	0.6259

NON-CAVITATION REGIME (ATTACHED TURBULENT FLOW)

The results for the non-cavitation turbulent flow regime are divided into 2 areas. The first section deals with single angle direction feed and the last section compound angle orifice design.

Single Angle Direction

Feed Impact of Orifice Variables on K_L – Since for each test the velocity ratio was held constant the data were initially analyzed using Equation 7. In all cases the results were consistent with that shown in Figure 11. For convenience $\rho V_2^2/2g$ in Equation 7 is termed the dynamic head.

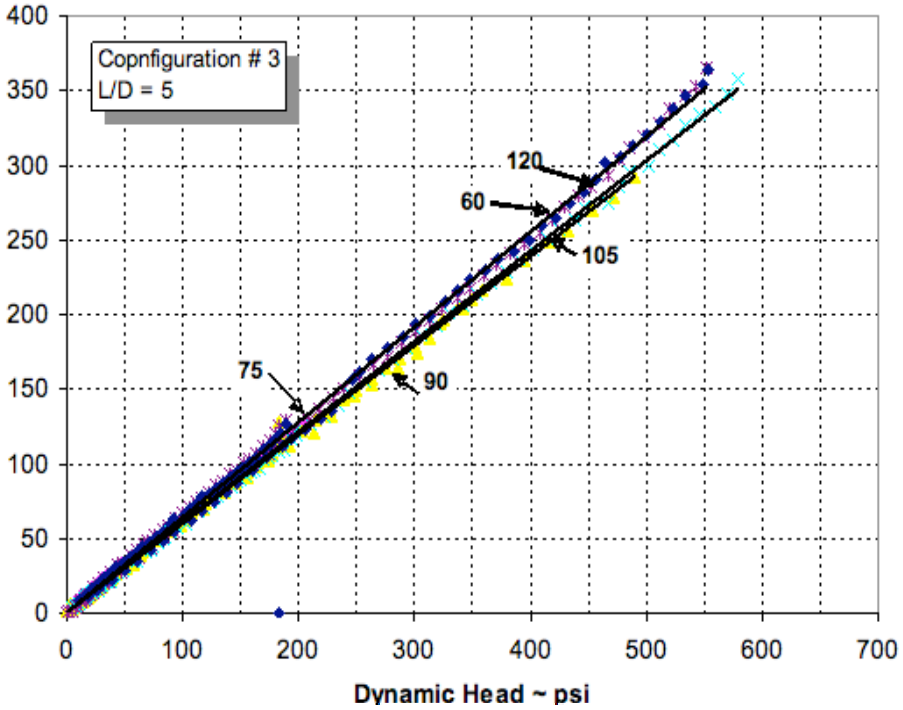

Figure 11 – Illustration of the Linearity of K_L with the Dynamic Head

For each test K_L was determined using Equation 7 utilizing the experimental data and the results are shown in Figure 12. The data fall in distinct patterns with K_L increasing with turning angle as well as manifold to orifice velocity ratio. This is consistent with expectations in that as (1) the manifold velocity increases the acceleration forces increase then energy losses should increase and (2) increasing turning angle should increase the turning loss coefficient, contraction coefficient, as well as the expansion losses. Since the data for each angle does not fit an exponential or log function the best fit equations for each angle tested are provided in Table 4 for convenience of analysis.

Of particular interest is that the intercept is ~ 0.6 as compared to an in-line orifice (i.e. with 0 cross velocity) of 0.5 for the contraction and expansion processes only. The difference is probably related to the friction (~0.01) and turbulence losses which at this velocity would be expected to be small.

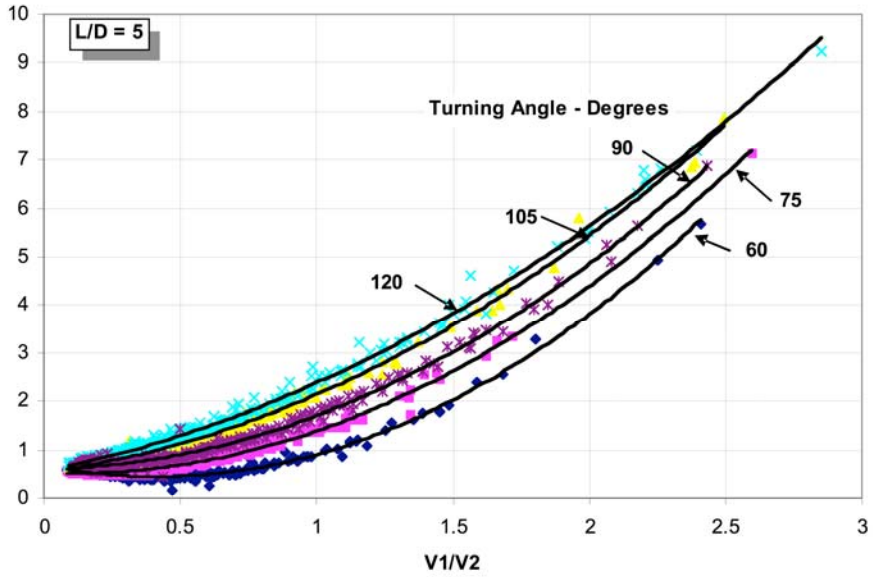

Figure 12 - Correlation of K_L for Differing Velocity Ratio and Turning Angle

Table 4 – Correlation Coefficients for Non-Cavitation Turbulent Flow

$$K_L = A\left(\frac{V_1}{V_2}\right)^2 + B\left(\frac{V_1}{V_2}\right) + C$$

ANGLE	A	B	C	R^2
60	1.3353	-1.1073	0.6787	0.9915
75	1.0708	-0.2061	0.5241	0.9877
90	1.028	0.0638	0.6118	0.9899
105	0.8496	0.7475	0.5415	0.9950
120	0.7143	1.106	0.5592	0.9956

The results from this study were also compared with pipe bending loss coefficients typically published in handbooks and fluid dynamics tests. Typical examples are:

45^o $K_L = 0.42$
90^o $K_L = .090$ rounded bend and 1.1 for R/D = 0
180^o $K_L = 2.2$

It is assumed that for constant area bends the bending loss is independent of Reynolds number. In fact, no discussion is found to suggest that K_L is not a constant. Since for our study K_L varies not only with bending angle but also with manifold to orifice velocity ratio, the results can not be directly compared. The comparison that was made was to compare the value of K_L for various V_1/V_2 ratios. This was accomplished by first plotting KL vs angle at constant velocity ratio then taking the average slope. The results

are plotted in Figure 13. A best fit linear line was used to show the trend. Note that as the velocity ratio is lowered the slope and value of K_L approaches that of the constant area bending loss coefficient. It would be expected that as the contraction and expansion losses are reduced the loss coefficient should approach that of a constant area bending value.

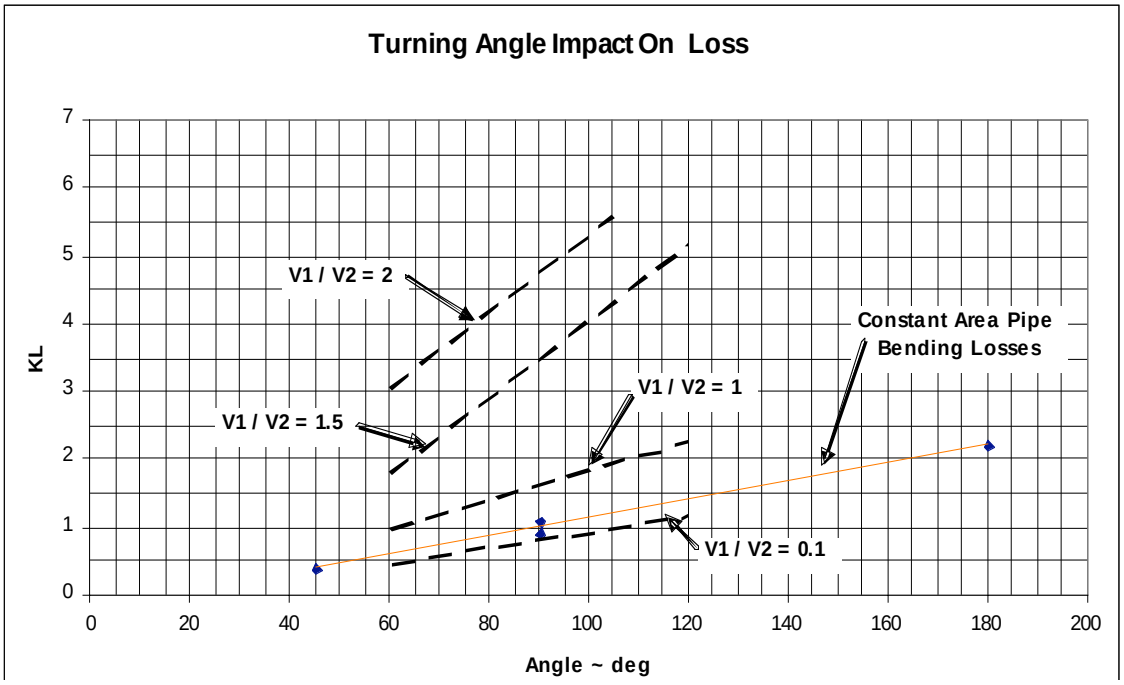

Figure 13 - Comparison of K_L between This Study and Constant Area Bending

The application of our results to predict orifice C_d is rather straight forward. Obviously the first step is similar to that described above utilizing the design information to determine that it does not fall within the cavitation regime. Once this is determined then K_L is determined from Figure 12 or the Equation and constants provided in Table 4, the head loss, H_L, is determined from Equation 9. Lastly, C_d is then calculated from Equation 2.

Compound Angle Direction Feed

Impact of Orifice Variables on K_L - The head loss coefficient, K_L, for the compound angle direction feed data was also determined as a function the manifold-to-orifice velocity ratio. The results are plotted in Figure 14 and compared with the 75 and 105 degree single direction results. As for the cavitation data the turbulent non-cavitation data also plot on a single curve for both the 60_90 and 75_90 orifices. However, for the non-cavitation regime the comparison suggests that while the 90^o turning angle appears to have the largest impact on head loss the orifice turning angle impacts can not be ignored.

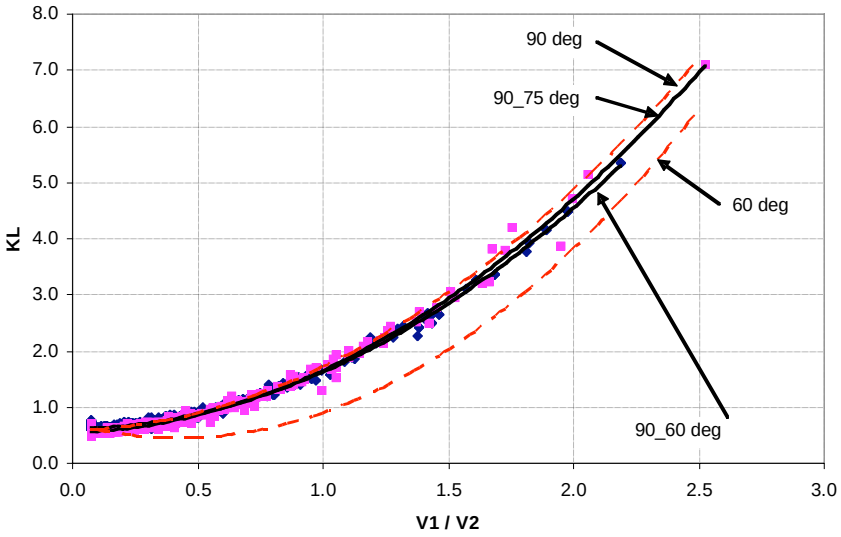

Figure 14 - Velocity Ratio Impact on K_L for Compound Angle Orifices

CONCLUSIONS

The results from this study demonstrate that the simple first order relationship between C_d and $K_{cav}^{1/2}$ as well as H_L and K_L are valid for non-axial orifices with cross flow and well as in-line orifices where cross velocity is 0. Also, correlations provided should aid designers in determining where cavitation will occur and define the Cc in addition to the head loss in the non-cavitation regime. Additional test efforts should be directed to extend the range of results to include L/D variation for all angles, inlet r/R, increased orifice angles for compound angles, and a larger range in orifice diameters as well as other fluids to define Reynolds number impacts. It is expected that the first order relationship will not be adequate for larger area ratios.

An attempt was made to reduce the individual equations for turning angle in both the cavitation and non-cavitation regime to a single equation. However the nonlinear nature of the equations did not produce a correlation with acceptable error.

The significant limitation for this study is that the manifold to orifice area ratio was not varied sufficiently to determine its impact. Therefore, the resulting correlations are valid only where the area ratio is sufficiently small that the term can be ignored.

The conclusions that can be drawn from the results presented are:

CAVITATION REGIME

- In the cavitation regime, C_c is controlled by the cavitation number

- When only part of the flow enters the orifice (i.e. cross velocity flow) the contraction coefficient is governed by both the turning angle and the velocity ratio V_1/V_2
- Inception of cavitation occurs at a K_{cav} of 1.8
- Full Cavitation occurs at a K_{cav} of ~ 1.5 to 1.8
- For the compound angle orifices C_c is more impacted by the initial 90^o turning angle than the orifice turning angle

NON-CAVITATION REGIME

- In the non-cavitation regime C_d is likely controlled by Reynolds number although in this study Re was only varied by velocity.
- The head loss coefficient K_L when only part of the manifold flow enters the orifice was found to be a function of both turning angle and velocity ratio V_1/V_c
- For the compound angle orifices K_L is more impacted by the initial 90^o turning angle than the orifice turning angle

.

NOMENCLATURE

SYMBOLS

A	Area in^2
Cc	Contraction Coefficient, A_2/A_1
Cd	Discharge Coefficient
H_L	Head Loss, lb/in^2
K	Loess coefficient
Kcav	Cavitation Number
P	Pressure, psi, psia
Re	Reynolds Number
V	Velocity, ft/sec
W	Flow Rate, lb/sec

GREEK

ρ	Liquid Density, lb/ft^3
θ	Turning Angle, degree

SUBSCRIPTS

1	Manifold
2	Orifice Exit
a	Contraction
c	Contraction
out	Flow rate, velocity, and pressure in the manifold
turb	Turbulence
f	Friction

REFERENCES

1. Nurick, W. H, ”Orifice Cavitation and its Effect on Spray Mixing”, Trans. ASME, J. Fluids Engineering, 7, 681-687, 1976
2. Nurick, W. H., Ohanian, T., Talley, D. and Strakey, P., “Impact of L/D on 90 Degree Sharp-Edge Orifice Flow with Manifold Passage Cross Flow”, Submitted to the Journal of Fluids Engineering (2007)
3. Martynov, S., Mason, D., And Heikal, M. ”Hydrodynamic Similarity of Cavitation Flows in Nozzles” Proc. 5th International Symposium on Multiphase Flow, Heat Mass Transfer and Energy Conversion, Xi’am, China 3-6 July 2005
4. Mishra, C. and Peles, Y. “Size Scale Effects on Cavitating Flows Through Microorifices Entrenched in Rectangular Microchannels”, J of Microelectromechanical Systems, V 14, No 55, October 2005
5. Heiniger, K. C., “Introduction to the Flow States in Water jet Systems” WJM – 2001, Krakow, 15.11.2001
6. Schmidt, D. P., Rutland, C J., and Corradini, M. L., “A Numerical Study of Cavitating Flow Through Various Nozzle Shapes”, SAE Paper 971597, 1997